

Interference Polarization in Magnetic Induction based Wireless Underground Sensor Networks

S. Kisseleff
Institute for Digital Communications
Friedrich-Alexander University
Erlangen-Nuremberg, Germany
Email: kisseleff@lnt.de

I. F. Akyildiz
Broadband Wireless Networking Lab
Georgia Institute of Technology
Atlanta, USA
Email: ian.akyildiz@ee.gatech.edu

W. Gerstaecker
Institute for Digital Communications
Friedrich-Alexander University
Erlangen-Nuremberg, Germany
Email: gersta@lnt.de

Abstract—Wireless Underground Sensor Networks (WUSNs) present a variety of new research challenges. For WUSNs, the goal is to establish an efficient wireless communication in the underground medium. A magnetic induction (MI) based transmission technique was proposed to overcome the very harsh conditions of the soil environment. In this paper, we investigate the potential of the MI-WUSNs if, in contrast to some previous proposals, no relays are used. Our main focus is on the throughput of the bottleneck link of the network, which corresponds to the overall network capacity. In order to reduce the number of relevant interferers and maximize the network throughput, we exploit the polarization of the used magnetic antennas (coils) by optimizing their orientation. Additional optimization of the system parameters improves the channel capacity of the bottleneck link. In addition, we consider a special case of the network deployment in mines and tunnels and propose a frequency switching scheme for better propagation conditions.

I. INTRODUCTION

Wireless underground sensor networks (WUSNs) are an emerging and promising research area. Typical applications for such networks include soil condition monitoring, earthquake prediction, communication in mines and tunnels, etc. [1], [2]. Since the propagation medium consists of soil, rock, and sand, traditional wireless signal propagation techniques using electromagnetic (EM) waves can be only applied for very small transmission ranges due to the high pathloss.

Magnetic induction (MI)-based WUSNs were first introduced in [2] and make use of magnetic antennas implemented as coils [3]. This approach is supposed to benefit from a low pathloss, hence, the transmission range can be greatly improved compared to the EM based approach.

The polarization of the EM waves is a well-known dimension which can be exploited to improve the system performance in terms of signal-to-interference-plus-noise-ratio (SINR), diversity, and throughput [4], [5], and [6]. In this work, we apply the polarization to the coils, which we model as dipoles. The polarization is used to avoid the interfering signals, which lead to a degradation of the SINR, such that in certain slots no reasonable transmission can be accomplished.

The network throughput, also called network capacity, was intensively studied in the past. Its most popular definition was originally given by [7]. This work was then extended to different types of wireless networks, such as cognitive radio networks [8], ad hoc networks with directional antennas [9], and magnetic induction based WUSNs [10]. In particular, [10] provides a scaling law for the MI based networks, adopting a channel model from [3] using several approximations, which

enables a simple calculation of the network throughput based on the general equations for wireless networks. As it was discussed in [11], [12], and [13], the channel capacity of an MI based link depends on the choice of the system parameters, like size of the coils and carrier frequency. A practical sensor network may contain several links of different lengths and therefore the optimal parameters may differ from link to link. In order to overcome the problems of individual manufacturing of each sensor node and switching between different connected links, which enables only half-duplex transmissions, one of our objectives in this work is the unification of these parameters, which results in a particular optimization problem, as described in Section III.

In this paper, we focus on tree-based networks with one sink, which collects the data from all nodes. The sink can be implemented as a node, which is connected wirelessly or via wireline with a mobile or removable aboveground device. This network structure is appropriate for most of the target applications with the primary goal of data collection. Each node transmits not only its own information, but also relays all received data from other nodes. We utilize the decode-and-forward relaying concept in this work. Also, we assume that no bit errors occur at the output of the decoder. In order to reduce the number of interferers and improve the channel capacity of the links, we design the network based on the minimum spanning tree, which can be found using the Prim algorithm [14]. As it was shown in [15], this approach establishes a network with a very good minimum channel capacity and throughput.

According to [7] and [10], the traffic load of a link equals the throughput of an information stream multiplied by the number of streams (routes) to be served by the node. In sensor networks it is frequently assumed that the data rates of all streams are equal. In order to avoid a bottleneck and loss of data packets, the traffic load has to be less or equal to the available data rate at the node corresponding to the channel capacity. However, the transmission may be disturbed by interfering signals coming from the other nodes. Hence, a multinode scheduling needs to be established, thus reducing the data rate. The transceivers are operated in full-duplex mode. A simultaneous transmission and reception of signals is possible, if the known (transmitted) signal is subtracted from the sum of transmitted and received signals at the load impedance, which is used for signal reception. In case of equality between the maximum available data rate and the traffic load, the throughput

of a link is given by [10] and [15]¹:

$$T_i = \frac{C_{ch,i}}{N_{routes,i} \cdot (1 + N_{interferers,i})}, \quad (1)$$

where $C_{ch,i}$ is the channel capacity of link i , $N_{routes,i}$ is the number of data streams of link i , $N_{interferers,i}$ is the number of interfering nodes, and T_i is the throughput of link i . The number of relevant interferer nodes for a particular link depends on the interference powers received from the different nodes, hence, on the system parameters like carrier frequency and polarization.

The paper is organized as follows. In Section II the network infrastructure of the MI-WUSN system is presented. In Section III the polarization of interfering signals and the choice of carrier frequency is investigated. Section IV provides insight into the simulation results and Section V concludes the paper.

II. FRAMEWORK

There are two strategies, which can be applied to the deployment of MI-based WUSNs [11]: MI-waveguides with a high coil density of around 1/(3 m) and direct MI transmission (no passive relays used). Due to a high relay density of the first strategy, the deployment effort becomes one of the crucial factors for the system rentability and reliability. As it was shown in [11], the channel capacity of the MI-waveguide based links can be very limited if the soil conditions in terms of conductivity and permittivity change. These changes cannot be avoided in most of the target applications. Also, it is a challenging task to deploy a large number of relay coils with exact orientation, since even a small deviation from the optimal coil orientation at any coil in the network can cause power reflections within the waveguide and lead to a disconnection of the whole network. If the second strategy is used, the resulting network is expected to be robust against both environmental changes and deviation of the coil orientation. Furthermore, the transmission range for the target applications is below 50 m, where the channel capacity of the direct MI transmission is larger than that of the MI-waveguides, as shown in [11]. However, due to the omnidirectional transmission and a good coupling between coils at low frequencies even for longer distances, the number of possible interferers is significantly higher than for using the first deployment strategy, yielding much lower throughput. In order to reduce the interference, we introduce the interference polarization, as also known from the literature for the conventional EM-wave based transmissions [5], [6]. In order to investigate the polarization of the magnetic field, we first model the transceiver coils as dipoles, which are placed in the far field of each other in a 3D space. The mutual inductance between the coils is then given by

$$M = \mu\pi N^2 \frac{a^4}{4r^3} \cdot J \cdot G, \quad (2)$$

where r denotes the distance between two coils, N stands for the number of coil windings, and a refers to the radius of the coil. G is an additional loss factor due to eddy currents, as

¹The interfering signals are separated by means of TDMA. Then, the own data is transmitted only in each $(1 + N_{interferers,i})$ slot and the maximal available data rate decreases by this factor.

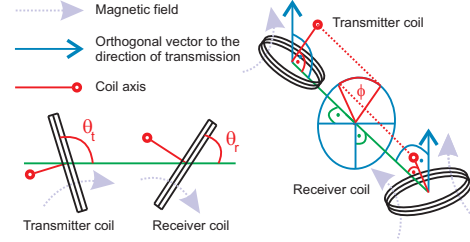


Fig. 1. Coil rotation and polarization angles.

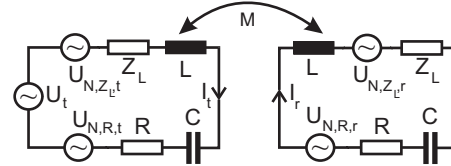


Fig. 2. MI-link circuit model: transmitter and receiver.

mentioned in [11], and J is the polarization factor. Note, that the well known polarization factor [10]

$$J_{2D} = 2 \sin(\theta_t) \sin(\theta_r) + \cos(\theta_t) \cos(\theta_r) \quad (3)$$

is only valid in the 2D space and therefore not fully applicable in our analysis. For the polarization factor in 3D space, it can be easily shown, that

$$J = J_{3D} = 2 \sin(\theta_t) \sin(\theta_r) + \cos(\theta_t) \cos(\theta_r) \cos(\phi), \quad (4)$$

where θ_t and θ_r are the angles between the coil radial directions and the line connecting the two coil centers, respectively. ϕ is the angle difference between the coil axes in the plane, which is orthogonal to the direction of transmission, see Fig. 1. We assume that all devices contain the same set of passive circuit elements, see Fig. 2. Each circuit includes a magnetic antenna (which is assumed to be a multilayer air core coil), a capacitor C , a resistor R (which models the copper resistance of the coil) and a load resistor Z_L in the transceivers. These passive elements are specified according to [11]. The capacitor is designed to make the circuits resonant at the carrier frequency $f_0 = \frac{1}{2\pi\sqrt{LC}}$. The load resistor Z_L is chosen to minimize the power reflection at the receiver. According to [11], this leads to $Z_L = R$ for the direct MI transmission. We assume that all devices are deployed in a conductive environment (soil) with constant properties over space and time.

We utilize the channel and noise models proposed in [11] for the calculation of channel capacity $C_{ch,i}$:

$$C_{ch,i} = \int_{-\infty}^{+\infty} \log_2 \left(1 + \frac{P_{t,i}(f)}{L_{p,i}(f) \cdot E\{P_N(f)\}} \right) df, \quad (5)$$

where $P_{t,i}(f)$ stands for the transmit power spectral density for link i and can be found via water filling with the total transmission power P per node. $E\{P_N(f)\}$ denotes the total noise power spectral density at the receiver of link i . The noise sources from the circuits of the surrounding devices can be neglected due to a high pathloss, yielding

$$E\{P_N(f)\} \approx \frac{1}{2} \frac{4KTZ_L^2}{\left| R + j2\pi fL + \frac{1}{j2\pi fC} + Z_L \right|^2}. \quad (6)$$

This noise is a thermal noise produced by the resistance Z_L . The pathloss of the link $L_{p,i}(f)$ can be calculated [11]

by taking into account the additional load impedance in the receiver:

$$L_{p,i}(f) = \frac{|S(x_i, x_{L,i}, 1)[S(x_i, x_{L,i}, 2) + x_{L,i}S(x_i, x_{L,i}, 1)]|}{|\text{Im}\{x_{L,i}\}|}, \quad (7)$$

$$S(x_i, x_{L,i}, k) = F(x_i, k) + x_{L,i} \cdot F(x_i, k-1),$$

$$F(x_i, k) = x_i \cdot F(x_i, k-1) + F(x_i, k-2),$$

$$F(x_i, 0) = 1, F(x_i, 1) = x_i,$$

where $x_{L,i} = \frac{R}{j2\pi f M_i}$ and $x_i = \frac{R+j2\pi f L + \frac{1}{j2\pi f C}}{j2\pi f M_i}$. In order to determine the number of the relevant interfering nodes, we first need to calculate the power of the interference signals, which is received by the target node. This interference power can be specified by

$$P_{I,j} = \int_{f_0-0.5B}^{f_0+0.5B} \frac{P_{t,I,j}(f)}{L_{p,I,j}(f)} df, \quad (8)$$

where $P_{t,I,j}(f)$ is the transmit power spectral density of the interference source j and $L_{p,I,j}(f)$ is the pathloss of the interfering signal from this source to the target receiver like in (7). In a practical system, the transmit power spectral density is chosen to maximize the channel capacity of the connected link by applying the water filling algorithm (this choice is still valid for the useful signal in this work as mentioned before). However, in order to guarantee a certain SINR, we assume the worst case, where $P_{t,I,j}(f)$ maximizes the interference power similar to [15]:

$$P_{t,I,j}(f) = \frac{1}{L_{p,I,j}(f)} \cdot \frac{P}{\int_{f_0-0.5B}^{f_0+0.5B} \frac{1}{L_{p,I,j}(f)} df}. \quad (9)$$

The receive power from the useful signal can be given similarly to (8):

$$P_{S,i} = \int_{f_0-0.5B}^{f_0+0.5B} \frac{P_{t,i}(f)}{L_{p,i}(f)} df, \quad (10)$$

where $P_{t,i}(f)$ results from the water filling algorithm to maximize the channel capacity of link i . The average received noise power can be calculated by integrating the noise power spectrum density in (6):

$$P_{\text{noise}} = \int_{f_0-0.5B}^{f_0+0.5B} E\{P_N(f)\} df. \quad (11)$$

A particular node j is selected as a relevant interferer and needs to be taken into account in scheduling, if $\frac{P_{S,i}}{P_{I,j} + P_{\text{noise}}} < \gamma$ with the SINR threshold $\gamma = 10$ dB in this work. The number of relevant interferers for a link i is stored in $N_{\text{interferers},i}$.

III. THROUGHPUT OPTIMIZATION

The optimization problem can be formulated as follows:

$$\begin{aligned} & \arg \max_{f_0, V \in \mathbb{R}^{3 \times N_{\text{nodes}}}} \min_i T_i, \\ \text{s.t.:} & P_i = P \quad \forall i, \end{aligned} \quad (12)$$

where f_0 is the carrier frequency (identical for all links) and N_{nodes} is the total number of nodes in a network. T_i is the throughput according to (1). In addition, we assume equal transmit power in all nodes (P_i : transmit power of i th node). The matrix V contains the direction vectors of the coils expressed in cartesian coordinates. As it is shown in [11], finding the optimal system parameters for maximizing

the channel capacity of an MI-link is a non-convex problem, which cannot be solved using convex optimization tools from [16]. Because the problem in [11] is obviously a subproblem of (12), (12) is also non-convex.

A. Optimal Carrier Frequency

Due to a large distance between the transceivers and therefore a very low mutual inductance of the direct MI transmission based links (7) can be approximated:

$$L_{p,i} \approx \left| \frac{R}{j2\pi f M_i} \right|^2. \quad (13)$$

As discussed in [11], the loss factor G in (2) can be determined according to $G = e^{-\frac{r}{\delta}}$, where δ denotes the skin depth. Due to the low optimal carrier frequency of the direct MI transmission, as results from [11], the approximation of the skin depth $\delta \approx \frac{1}{\sqrt{f_0 \pi \sigma \mu}}$ is valid. Hence, the pathloss in (13) close to the carrier frequency can be minimized, if $|j2\pi f_0 M_i|$ is maximized, yielding

$$f_0 M_i = f_0 \cdot \mu \pi N^2 \frac{a^4}{4r_i^3} J_i \cdot e^{-r/\delta} \approx f_0 \cdot \mu \pi N^2 \frac{a^4}{4r_i^3} J_i \cdot e^{-r_i \sqrt{f_0 \pi \sigma \mu}}. \quad (14)$$

The maximum of this function with respect to f_0 is given by

$$f_0 = \left(\frac{2}{r_i \sqrt{\pi \sigma \mu}} \right)^2. \quad (15)$$

However, due to the different lengths of the links, the optimal carrier frequency is a tradeoff between the different optimal frequencies of all available links. The search for the optimal frequency should be therefore performed in the range $[f_{\min}, f_{\max}] = \left[\left(\frac{2}{r_{\max} \sqrt{\pi \sigma \mu}} \right)^2, \left(\frac{2}{r_{\min} \sqrt{\pi \sigma \mu}} \right)^2 \right]$, where r_{\min} and r_{\max} denote the minimum and maximum transmission distance in the network, respectively. In this range, a grid is spanned and the optimal orientation of all coils in the network can be found by applying a discrete search as described in Section III-B for each point of the grid. The point with the largest throughput indicates the best carrier frequency.

B. Network Polarization

The throughput of the network can be greatly improved, if the number of interfering nodes is reduced. We exploit the polarization property of the coils, in order to reduce the number of relevant interferers. The motivation for this technique is due to the fact, that the polarization factor J from (4) becomes zero for several combinations of the angles θ_t , θ_r , and ϕ , e.g. if $\theta_t = 0$ and $\theta_r = \pi/2$. As it was mentioned before, a high deployment effort may lead to certain deviations in the orientation and position of the deployed coils. We assume that for an accurate deployment an angle separation of at least 45° between two closest possible directions is needed. This ensures, that small deviations from the optimal directions become negligible and do not change the system behaviour. A map of possible directions can be then visualised using a cube, like in Fig. 3. The coordinates of each colored point are specified in the space given by the basic vectors \vec{a} , \vec{b} , and \vec{c} , and correspond to a possible direction of the coil. Obviously, there are 9 pairs of points². For each pair, the

²In Fig. 3, every two points, which belong to the same pair, are marked with the same color.

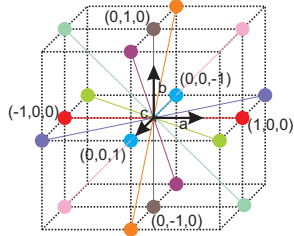


Fig. 3. Possible coil axes' directions.

two points correspond to the opposite directions on the same axis. Therefore, the absolute value of the polarization factor and the pathloss according to (13) remain the same, and the total number of different constellations is 9.

The optimal solution for the orientation of the coils can be found by applying a full search over all possible combinations. This leads to a total amount of $9^{N_{\text{nodes}}}$ computations. Due to the non-convexity of the original problem, it is not possible to determine the solution without taking into consideration all possible constellations. However, the computation effort increases exponentially with the number of nodes in a network, such that the optimization becomes impractical for a network with $N_{\text{nodes}} > 10$.

C. Polarization Algorithm

We propose an iterative algorithm for improving the minimum throughput defined in (1). For this, we start with the calculation of the throughput metric for all links with the coils rotated to the surface (default state). The link with the least throughput is selected as the worst link and the minimum throughput is stored for performance comparison.

At first, we define the basic vectors \vec{a} , \vec{b} , and \vec{c} . Assuming, that one of the vectors, e.g. \vec{a} , is identical with the transmission direction of the worst link, we make sure that this worst link can be improved at least by the horizontal axes deployment gain [11] (the polarization factor in (4) and therefore the mutual inductance in (2) double compared to the vertical axes deployment). We choose the second vector (e.g. \vec{b}) to show to the ground surface, yielding the original constellation to be available as well. The third vector \vec{c} is then orthogonal to the given vectors \vec{a} and \vec{b} .

In each iteration, the closest N_x ($N_x = 5$ in this work) nodes to the receiver node of the worst link and the receiver node itself are selected and for these nodes all 9^{N_x} constellations are investigated. The optimal combination is found, which maximizes the least throughput metric among all links of the network. The corresponding link is selected for the next iteration. This strategy ensures a monotonic increase of the throughput from step to step. The algorithm stops, if the worst link remains the same as the original worst link of this iteration, which means, that no further gain can be achieved.

IV. NUMERICAL RESULTS

In this section, we discuss numerical results for the network throughput. In our simulations, we assume a total transmit power of $P = 10$ mW per node. We assume a square field of the size $F_x \times F_x$ with $F_x = 100$ m in this work. Within this field, a random uniformly distributed set of N_{nodes} sensor

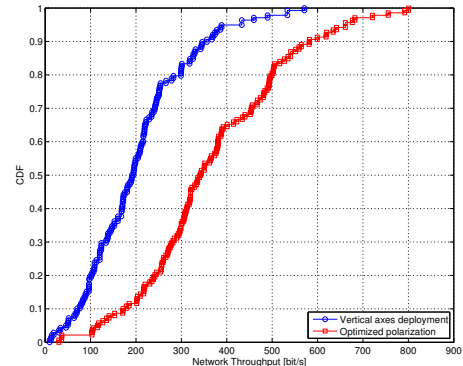


Fig. 4. Cumulative distribution of the network throughput for WUSNs.

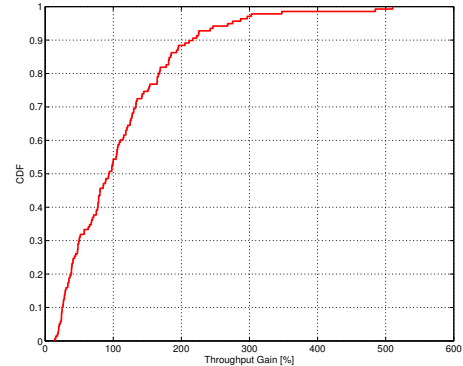


Fig. 5. Throughput gain using the interference polarization.

nodes ($N_{\text{nodes}} = 10$ in this work) is acquired for each network optimization. In this set, a root node is selected, which is the closest node to the lower left field corner. We utilize coils with wire radius 0.5 mm, coil radius 0.15 m, and 1000 windings. The conductivity and permittivity of dry soil are, respectively, $\sigma = 0.01$ S/m and $\epsilon = 7\epsilon_0$, where $\epsilon_0 \approx 8.854 \cdot 10^{-12}$ F/m. Since the permeability of soil is close to that of air, we use $\mu = \mu_0$ with the magnetic constant $\mu_0 = 4\pi \cdot 10^{-7}$ H/m.

For the performance evaluation, we show a cumulative distribution function of the network throughput for random networks using the vertical deployment scheme (if all coil axes are turned to the ground surface) and the proposed coil axes optimization, see Fig. 4. Obviously, a significant throughput gain can be obtained, if the coils' axes are chosen properly. Furthermore, in order to quantify the performance improvement, we also show the relative throughput gain. As shown in Fig. 5, with probability of $\approx 50\%$ a throughput gain of more than 100% results, which means the doubling of the throughput. With probability of $\approx 13\%$ the gain is more than 200%. On average, a gain of 110% can be expected.

Although the main focus of this work is on network optimization for the WUSNs, we want to investigate the potential of the MI based WSNs, which are deployed in less challenging environments. One possible application for such WSNs is a communication system in mines and tunnels, where the usual propagation properties for the Line-of-Sight (LoS) transmissions are close to the free-space propagation ("Aboveground Mode"). However, after a possible disaster event, the propagation medium may become conductive and the network should be able to switch to the "Underground Mode", which can be done automatically using a different set of

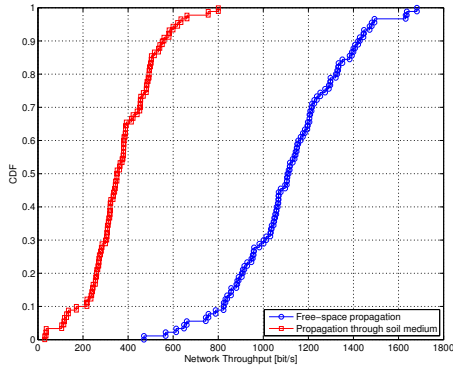


Fig. 6. Network throughput before and after the disaster in mines.

capacitors for operations at lower frequencies. The switching of the mode is triggered by the channel estimation process. Once a particular node recognizes an abrupt change in the propagation characteristics, an alert is issued and the remaining nodes are notified by the link nodes connected to them. This alert message is easily implemented and detected due to the utilized decode-and-forward relaying concept. For simplicity, we assume, that the position and orientation of the devices remains unchanged during and after the event. Otherwise, the probability of the deviation of polarization needs to be investigated, which is out of the scope of this work. For the “Aboveground Mode”, the free-space propagation can be assumed, yielding the scaling factor $G = 1$ in (2), because the losses due to the medium are negligible. As it was pointed out in [11], there is a lower bound for the choice of the capacitance of the capacitor C_0 , which is motivated by the parasitic effects in capacitors and coils, see [11]. In this work, $C_0 = 1$ pF is utilized. Due to the monotonic increase of magnetic induction with the carrier frequency, the latter is bounded by $f_0 = \frac{1}{2\pi\sqrt{LC_0}}$, which is therefore the optimal carrier frequency. For comparison, we show the network throughput of the optimized polarization for the free-space propagation and for the propagation through the soil medium, see Fig. 6. Due to the losses in the medium for the “Underground Mode”, the resulting network throughput is lower than it was before the disaster in “Aboveground Mode”. However, due to a proper choice of the carrier frequency, as described before, and due to the interference polarization based deployment, it is still possible to provide sufficient data rate even for this case. In Fig. 7, the throughput loss is shown. For 35% of cases the loss for the polarization optimization is larger than for the default scheme, which means that the default scheme is less vulnerable to the environmental changes. However, it can be shown that for these cases the throughput gain of the polarization technique is large as well, such that the proposed scheme is still beneficial. In addition, for the remaining and most crucial losses ($\approx 65\%$ of cases), the proposed technique is more beneficial, too. The mean throughput loss is for both constellations similarly $\approx 66\%$.

V. CONCLUSION

In this paper we investigated the polarization of the coils and exploited it to minimize the interference and increase the channel capacity of the MI based links. A significant increase of the network throughput is observed for the proper choice of

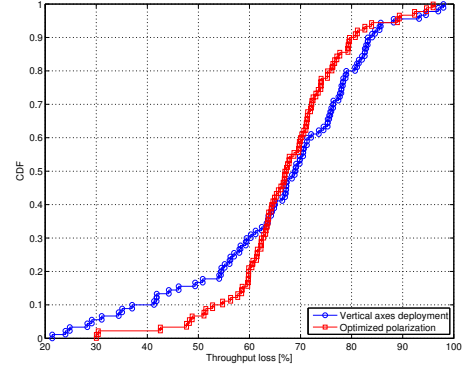


Fig. 7. Throughput loss due to disaster in mines.

the coils’ axes directions. This makes the proposed scheme inevitable for stationary deployed MI based networks. In addition, we considered a network, which can be deployed in mines and tunnels. For the case of a sudden disaster event, we propose a mode switching scheme, which optimizes the propagation conditions before and after the event. We observe, that even after the disaster event, a substantial network throughput can be guaranteed, if the interference polarization is applied.

REFERENCES

- [1] I.F. Akyildiz, W. Su, Y. Sankarasubramaniam, and E. Cayirci, “Wireless sensor networks: A survey,” *Comput. Netw. J.*, vol. 38, pp. 393–422, March 2002.
- [2] I.F. Akyildiz and E.P. Suntebeck, “Wireless underground sensor networks: Research challenges,” *Ad Hoc Netw. J.*, vol. 4, pp. 669–686, July 2006.
- [3] Z. Sun and I.F. Akyildiz, “Magnetic induction communications for wireless underground sensor networks,” *IEEE Trans. on Antennas and Propag.*, vol. 58, pp. 2426–2435, July 2010.
- [4] T. Svantesson, M.A. Jensen, and J.W. Wallace, “Analysis of electromagnetic field polarizations in multiantenna systems,” *IEEE Trans. on Wireless Communications*, vol. 3, no. 2, pp. 641–646, March 2004.
- [5] D.P. Stapor, “Optimal receive antenna polarization in the presence of interference and noise,” *IEEE Trans. on Antennas and Propag.*, vol. 43, no. 5, pp. 473–477, May 1995.
- [6] B.T. Walkenhorst and T.G. Pratt, “Polarization-based interference mitigation for OFDM signals in channels with polarization mode dispersion,” in *Proc. of MILCOM’08*, November 2008.
- [7] P. Gupta and P.R. Kumar, “The capacity of wireless networks,” *IEEE Trans. on Information Theory*, vol. 46, pp. 388–404, March 2000.
- [8] C.X. Wang, X. Hong, H.H. Chen, and J. Thompson, “On capacity of cognitive radio networks with average interference power constraints,” *IEEE Trans. on Wireless Communications*, vol. 8, pp. 1620–1625, April 2009.
- [9] A. Spyropoulos and C.S. Raghavendra, “Capacity bounds for ad-hoc networks using directional antennas,” in *Proc. of IEEE ICC’03*, May 2003.
- [10] Z. Sun and I.F. Akyildiz, “On capacity of magnetic induction-based wireless underground sensor networks,” in *Proc. of IEEE INFOCOM’12*, March 2012, pp. 370–378.
- [11] S. Kisseleff, W.H. Gerstacker, R. Schober, Z. Sun, and I.F. Akyildiz, “Channel capacity of magnetic induction based wireless underground sensor networks under practical constraints,” in *Proc. of IEEE WCNC’13*, April 2013.
- [12] H. Jiang and Y. Wang, “Capacity performance of an inductively coupled near field communication system,” in *IEEE International Symposium of Antenna and Propagation Society*, July 2008.
- [13] J.I. Agbinya and M. Mashipour, “Power equations and capacity performance of magnetic induction communication systems,” *Wireless Personal Communications Journal*, vol. 64, no. 4, pp. 831–845, 2012.
- [14] R.C. Prim, “Shortest connection networks and some generalizations,” *Bell Sys. Tech. J.*, pp. 1389–1401, November 1957.
- [15] S. Kisseleff, W. Gerstacker, Z. Sun, and I.F. Akyildiz, “On the throughput of wireless underground sensor networks using magneto-inductive waveguides,” in *Proc. of IEEE Globecom’13 (accepted for publication)*, 2013.
- [16] S. Boyd and L. Vandenberghe, *Convex Optimization*. Cambridge University Press, 2004.